J Therm Anal Calorim (2010) 101:561–566
DOI 10.1007/s10973-010-0848-z

Formation and properties of the new $Al_8V_{10}W_{16}O_{85}$ and $Fe_{8-x}Al_xV_{10}W_{16}O_{85}$ phases with the M–Nb_2O_5 structure

Piotr Tabero

CCTA10 Special Issue

Abstract A new, previously unknown phase $Al_8V_{10}W_{16}O_{85}$ has been obtained from reaction taking place in the solid state. It forms continuous solid solution with $Fe_8V_{10}W_{16}O_{85}$ of the $Fe_{8-x}Al_xV_{10}W_{16}O_{85}$ general formula. All these phases are isostructural with M–Nb_2O_5 and $(W_{0.35}V_{0.65})_2O_5$ and belong to a block structure phases with ReO_3 type blocks of $4 \times 4 \times \infty$ dimensions. $Al_8V_{10}W_{16}O_{85}$ is tetragonal and has the lattice constants $a = b = 1.9487(1)$ nm and $c = 0.36706(4)$ nm. It melts incongruently at 1,183 K depositing $Al_2(WO_4)_3$ and WO_3. The increase of the Al^{3+} ions content in the crystal lattice of $Fe_8V_{10}W_{16}O_{85}$ causes the melting point increasing, and decreasing of $a = b$ unit cell parameters with c being almost constant. IR spectra of $Al_8V_{10}W_{16}O_{85}$ and $Fe_{8-x}Al_xV_{10}W_{16}O_{85}$ phases have been recorded.

Keywords $Al_8V_{10}W_{16}O_{85}$ · $Fe_{8-x}Al_xV_{10}W_{16}O_{85}$ solid solution · DTA-TG · XRD · IR

Introduction

The oxidative dehydrogenation (ODH) of light hydrocarbons and selective reduction of NO with NH_3 have been extensively studied over alumina or titania supported vanadium oxide catalysts [1–4]. A major challenge in the light hydrocarbons ODH catalytic technology is improvement in the alkene yields, because significant carbon oxide byproducts are also formed. One method to improve the yield of the desired product is to use metal oxide additives. The vanadium containing catalysts can be tuned with second or third component like Mo, W, Sb, Ni, and Co [1–4]. The effect of the incorporation of second or third component to V-containing catalysts results in a replace of the polyvanadate structure with less reactive V–O–X structure, leading to lower reducibility and oxidative dehydrogenation rates. In spite of extensive scientific studies on catalytic activity of multicomponent oxide systems, the knowledge on phase equilibria being established in an appropriate ternary or quaternary systems is unsatisfactory. In the case of Al_2O_3–V_2O_5–WO_3 only binary systems have been the subject of investigations. In the Al_2O_3–WO_3 system a phase with general formula $Al_2(WO_4)_3$ forms, crystallizing in an orthorhombic system and melting congruently at 1,527 K [5, 6]. Whereas in the Al_2O_3–V_2O_5 system triclinic $AlVO_4$ forms, being isostructural with $FeVO_4$ [7]. $AlVO_4$ melts incongruently at 1,018 K with deposition of α-Al_2O_3 as a solid product [7]. Literature data pertaining V_2O_5–WO_3 imply that only solid solution of the $V_{2-x}W_xO_5$ type with a $x < 0.07$ [8] or $x \leq 0.15$ [9] solubility limit is formed. On the other hand, the Fe_2O_3–V_2O_5–WO_3 system has been the subject of extensive studies [10–16]. The components of this system react with each other to form $Fe_8V_{10}W_{16}O_{85}$ phase [10–12]. $Fe_8V_{10}W_{16}O_{85}$ crystallizes in a tetragonal system [13], but its structure is unknown. This compound melts at 1,103 K with depositing two solid products, i.e. Fe_2WO_6 and WO_3 [10]. Besides, a solid solution of V_2O_5 in Fe_2WO_6 has been found to occur in the three-component system [11]. It is also known that in the quaternary system Fe_2O_3–V_2O_5–WO_3–MoO_3 $Fe_8V_{10}W_{16-x}Mo_xO_{85}$ solid solution is formed

P. Tabero (✉)
Department of Inorganic and Analytical Chemistry, West Pomeranian University of Technology, Szczecin, Al. Piastow 42, 71-065 Szczecin, Poland
e-mail: ptab@ps.pl

(for $x \leq 4$), isostructural with $Fe_8V_{10}W_{16}O_{85}$ [14]. The equal charge and close values of Fe^{3+} and Al^{3+} ionic radii ($R_{Al} = 0.0535$ nm and $R_{Fe} = 0.0645$ nm in octahedral coordination), let one expect formation of solid solutions as a result of substitution of aluminum for iron in the quaternary Fe_2O_3–Al_2O_3–V_2O_5–WO_3 system. This study shows the experimental results of the substitution of aluminum for iron in the case of $Fe_8V_{10}W_{16}O_{85}$ compound.

Experimental

The following materials were used for the research: V_2O_5, p.a. (POCh, Poland), WO_3, 99.9% (Fluka AG, USA), Al_2O_3, pure (POCh, Poland), α-Fe_2O_3 p.a. (POCh, Poland), MoO_3, pure (POCh, Poland), ZnO 99.9% (Sigma–Aldrich, Germany), and $CoCO_3$, pure (POCh, Poland).

For the experiments five samples were selected with contents corresponding to $Fe_{8-x}Al_xV_{10}W_{16}O_{85}$ formula with $x = 0, 2, 4, 6$, and 8. They represented the whole component concentration range of the system: $Fe_8V_{10}W_{16}O_{85}$–$Al_8V_{10}W_{16}O_{85}$. The content of V_2O_5 and WO_3 in the all mixtures was always constant and amounted to 20.00 and 64.00 mol%, respectively. The oxides weighed in suitable proportions were homogenized and calcinated at 873, 923, 973, 1023, and 1073 K in 24 h stages. After each sintering stage the samples were powdered using agate mortar and examined with the aid of XRD. The samples obtained after last heating stage were additionally examined by the IR and DTA/TG methods. Results of investigations by XRD, DTA, and IR methods allow a determination of phase composition of samples, establishing of their melting temperatures as well as melting behavior [17–20].

Two additional samples were prepared for IR investigations. ZnV_2O_6 was synthesized from oxides by sintering in 24 h stages at 823, 873, and 923 K, whereas $CoMoO_4$ from $CoCO_3$ and MoO_3 by calcination at 873, 923, and 973 K.

The DTA/TG examinations were made using an apparatus of Paulik–Paulik–Erdey type (MOM, Hungary). Samples of 500 mg were investigated in air up to the 1,273 K in quartz crucibles and at the heating rate of 10 K min^{-1}.

X-ray diffraction phase analysis of the samples was performed using a DRON-3 diffractometer (Bourevestnik, Sankt Petersburg, Russia) applying the CoKα/Fe radiation (step 0.02° 2θ, time 1 s).

The IR spectra were recorded on a SPECORD M-80 spectrometer (Carl-Zeiss Jena, Germany) in the wavenumber region of 1,500–200 cm^{-1}. The samples were mixed with KBr in a wieght ratio of 1:300 and then pressed to pellets.

Results and discussion

The XRD experimental results have shown that diffraction patterns of all materials after the last calcination stage at 1,073 K, were similar to one another and to the diffractogram of $Fe_8V_{10}W_{16}O_{85}$ both with respect to the number and to the mutual intensity relations of the recorded diffraction lines. The angular positions of these lines were shifted with increasing the Al_2O_3 content in initial oxide mixtures toward higher angles 2θ, in comparison with the diffractogram of $Fe_8V_{10}W_{16}O_{85}$, i.e., they corresponded to smaller interplanar distances d. The same tendency was observed in the case of formation of solid solution of the $Fe_8V_{10}W_{16-x}Mo_xO_{85}$ type (for $x \leq 4$) when the Mo^{6+} ions were substituted for W^{6+} ones [14]. The obtained results indicated that continuous substitutional solid solution of a general formula $Fe_{8-x}Al_xV_{10}W_{16}O_{85}$ is formed by an incorporation of the Al^{3+} ions into the crystal lattice of $Fe_8V_{10}W_{16}O_{85}$ instead of Fe^{3+}. The formulae of obtained solid solution were evaluated from the content of initial oxides. Diffraction lines of the $Al_8V_{10}W_{16}O_{85}$ and $Fe_{8-x}Al_xV_{10}W_{16}O_{85}$ type solid solution samples ($x = 2, 4, 6$) recorded within 2θ ($CoK_{\alpha\text{-aver}}$) 4–65° region were selected for indexing (program Refinement). The result of indexing of powder diffraction pattern of $Al_8V_{10}W_{16}O_{85}$ is presented in Table 1. The parameters and volumes of the unit cells of

Table 1 The result of indexing of X-ray powder diffraction pattern of the $Al_8V_{10}W_{16}O_{85}$

No **1**	d_{exp}/nm **2**	d_{calc}/nm **3**	*h k l* **4**	100 I **5**
1	1.3777	1.3779	1 1 0	1
2	0.6899	0.6890	2 2 0	4
3	0.4594	0.4593	3 3 0	40
4	0.3608	0.3607	1 0 1	75
5	0.3444	0.3445	4 4 0	100
6	0.3383	0.3383	2 1 1	9
7	0.3249	0.3248	6 0 0	3
8	0.3036	0.3037	3 2 1	3
9	0.2756	0.2756	7 1 0	7
10	0.2672	0.2672	4 3 1	76
11	0.2576	0.2577	5 2 1	2
12	0.2436	0.2436	8 0 0	12
13	0.2342	0.2343	5 4 1	2
14	0.2298	0.2297	6 6 0	2
15	0.2218	0.2218	7 0 1	14
16	0.2018	0.2019	8 1 1	4
17	0.1969	0.1969	7 7 0	28
18	0.1836	0.1835	0 0 2	16
19	0.1809	0.1809	10 4 0	3
20	0.1723	0.1722	8 8 0	3

Table 2 Unit cell parameters and volumes of M–Nb_2O_5 [21], $(W_{0.35}V_{0.65})_2O_5$ [22], $Fe_8V_{10}W_{16}O_{85}$ [13], $Fe_8V_{10}W_{12}Mo_4O_{85}$ [14], $Al_8V_{10}W_{16}O_{85}$, and $Fe_{8-x}Al_xV_{10}W_{16}O_{85}$ solid solution ($x = 2, 4, 6$)

No.	Formula	$a = b$/nm	c/nm	V/nm^3
1	M–Nb_2O_5	2.044	0.3832	1.6001
2	$(W_{0.35}V_{0.65})_2O_5$	1.9506 (1)	0.37039 (7)	1.4093
3	$Al_8V_{10}W_{16}O_{85}$	1.9487 (1)	0.36706 (4)	1.3939
4	$Al_6Fe_2V_{10}W_{16}O_{85}$	1.9553 (3)	0.3684 (2)	1.4103
5	$Al_4Fe_4V_{10}W_{16}O_{85}$	1.9614 (2)	0.36958 (6)	1.4215
6	$Al_2Fe_6V_{10}W_{16}O_{85}$	1.9674 (4)	0.3705 (2)	1.4338
7	$Fe_8V_{10}W_{16}O_{85}$	1.9753 (3)	0.3717 (2)	1.4503
8	$Fe_8V_{10}W_{12}Mo_4O_{85}$	1.9725 (6)	0.3713 (5)	1.4446

$Al_8V_{10}W_{16}O_{85}$ as well as $Fe_8V_{10}W_{12}Mo_4O_{85}$ [14] and $Fe_{8-x}Al_xV_{10}W_{16}O_{85}$ solid solutions are presented in Table 2.

Looking for isostructural compounds with $Fe_8V_{10}W_{16}O_{85}$, $Al_8V_{10}W_{16}O_{85}$, $Fe_{8-x}Al_xV_{10}W_{16}O_{85}$, and $Fe_8V_{10}W_{16-x}Mo_xO_{85}$ solid solution phases it have been taken under consideration that their general formulas can be given as $M_{34}O_{85}$ or $17 \times M_2O_5$ (M stands for metal ion) and that these compounds have very characteristic values of unit cell parameters. The literature scan has shown that all these phases are isostructural with polymorphic form of niobium(V) oxide designated as M–Nb_2O_5 [21] and $(W_{0.35}V_{0.65})_2O_5$, (M_2O_5) [22]. The values of their unit cell parameters (Table 2), the same type of general formula, M_2O_5, as well as very similar powder diffraction patterns support this assumption. Figure 1 presents the crystal structure of M–Nb_2O_5 [21]. M–Nb_2O_5 and $(W_{0.35}V_{0.65})_2O_5$ belong to a block structure phases with ReO_3 type blocks of $4 \times 4 \times \infty$ dimensions. These phases are built up of corner and edge shared highly distorted MO_6 octahedra. An analysis of the data compiled in Table 2 indicates that with increasing the incorporation extent of the smaller Al^{3+} ions into the $Fe_8V_{10}W_{16}O_{85}$ structure, the unit cell parameters $a = b$ are decreasing whereas parameter c being almost constant.

The single phase materials obtained after the last heating stage were subjected to the DTA/TG investigation. In the DTA curve of $Fe_8V_{10}W_{16}O_{85}$ two endothermic effects were recorded up to 1,273 K with their onsets at 1,113 and 1,213 K. The second effect was much smaller than the first one and it was registered as a poorly pronounced remnant effect. It was in accord with literature data where the first endothermic effect was attributed to incongruent melting of $Fe_8V_{10}W_{16}O_{85}$ [10].

On the other hand in the DTA curves of the $Fe_{8-x}Al_xV_{10}W_{16}O_{85}$ solid solution materials ($x > 0$) and $Al_8V_{10}W_{16}O_{85}$ phase one endothermic effect was recorded up to 1,273 K. Figure 2 shows the DTA curve of $Al_8V_{10}W_{16}O_{85}$. The onset temperature of the endothermic effects was increasing gradually with the increase of aluminum content. Values of temperatures were 1163, 1168, 1173, and 1183 K for $x = 2$, 4, 6, and 8, respectively. No weight changes were recorded on the TG curves (not presented) up to the onsets of the observed endothermic effects on the DTA curves.

In order to explain the nature of the endothermic effect on the DTA curve of $Al_8V_{10}W_{16}O_{85}$ and to establish its melting behavior the sample of this phase was additionally heated for 3 h at 1,213 K, i.e., at temperature close to the extremum temperature of the endothermic effect registered in the DTA curve. After heating at 1,213 K sample was cooled rapidly to room temperature. The X-ray phase

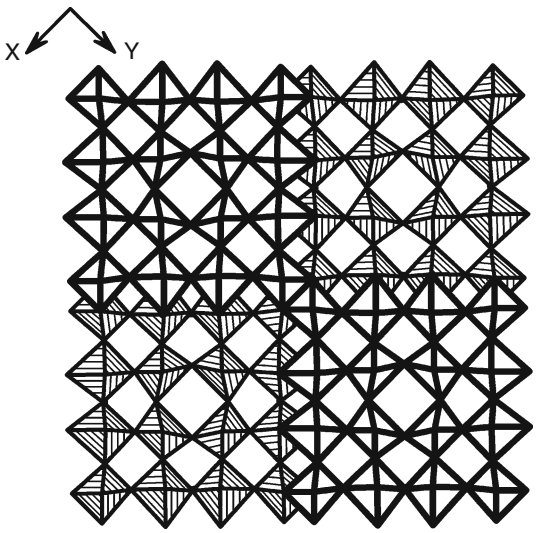

Fig. 1 The crystal structure of M–Nb_2O_5 [21]

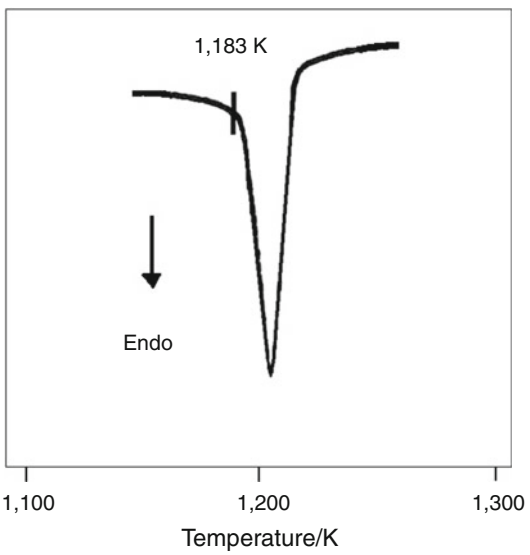

Fig. 2 DTA curve of $Al_8V_{10}W_{16}O_{85}$

analysis of the partially melted at this temperature sample (Fig. 3, graph *b*) showed that it comprised a mixture of WO_3, $Al_2(WO_4)_3$, and V_2O_5. Diffraction lines characteristic for V_2O_5 were shifted toward higher 2θ angles indicating formation of $V_{2-x}M_xO_5$ (M stands for metal ion) solid solution. At 1,213 K V_2O_5 do not exist already as solid phase, so it crystallizes from the liquid. Thus, it was concluded that $Al_8V_{10}W_{16}O_{85}$ melts incongruently and the solid products of its melting are WO_3 and $Al_2(WO_4)_3$:

$$Al_8V_{10}W_{16}O_{85(s)} \rightarrow WO_{3(s)} + Al_2(WO_4)_{3(s)} + \text{liquid}$$

$Fe_8V_{10}W_{16}O_{85}$, $Al_8V_{10}W_{16}O_{85}$ as well as the solid solution phases $Fe_8V_{10}W_{16-x}Mo_xO_{85}$ and $Fe_{8-x}Al_xV_{10}W_{16}O_{85}$ were also subjected to an investigation with the use of infra-red spectroscopy (IR). The results of literature survey [21, 22] have revealed that $Fe_8V_{10}W_{16}O_{85}$ type phases are isostructural with M–Nb_2O_5 and $(W_{0.35}V_{0.65})_2O_5$, built up from highly distorted MO_6 octahedra. Since the VO_6 octahedra are relatively less common polyhedra, for comparison, IR investigations have been conducted also in the case of ZnV_2O_6. The crystal structure of this phase is built up from distorted VO_6 octahedra [23]. On the other hand, IR spectrum of $CoMoO_4$ have been recorded because this phase has crystal structure related to these ones of M–Nb_2O_5 and $(W_{0.35}V_{0.65})_2O_5$ [24].

Figure 4 shows the IR spectra of $CoMoO_4$ (curve *a*), $Al_8V_{10}W_{16}O_{85}$ (curve *b*), $Fe_4Al_4V_{10}W_{16}O_{85}$ (curve *c*), $Fe_8V_{10}W_{16}O_{85}$ (curve *d*) [12], $Fe_8V_{10}W_{12}Mo_4O_{85}$ (curve *e*) [14], and ZnV_2O_6 (curve *f*).

The IR spectra of all $Fe_8V_{10}W_{16}O_{85}$ type phases are very similar, what supports assumption that these phases are isostructural.

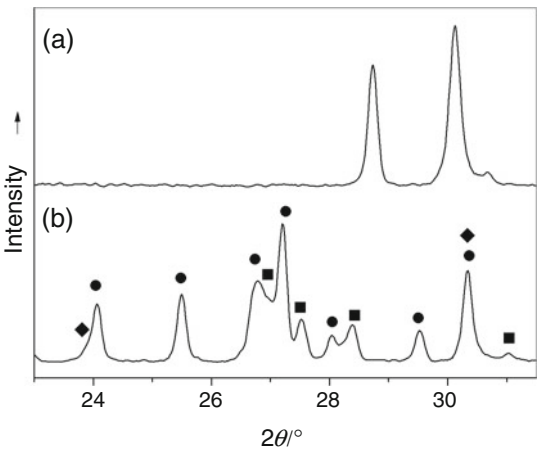

Fig. 3 Powder diffraction patterns of: (*a*) $Al_8V_{10}W_{16}O_{85}$, (*b*) sample of $Al_8V_{10}W_{16}O_{85}$ additionally heated for 3 h at 1,213 K and cooled rapidly to room temperature comprised a mixture of WO_3 (*filled square*), $Al_2(WO_4)_3$ (*filled circle*) and $V_{2-x}M_xO_5$ (*filled diamond*)

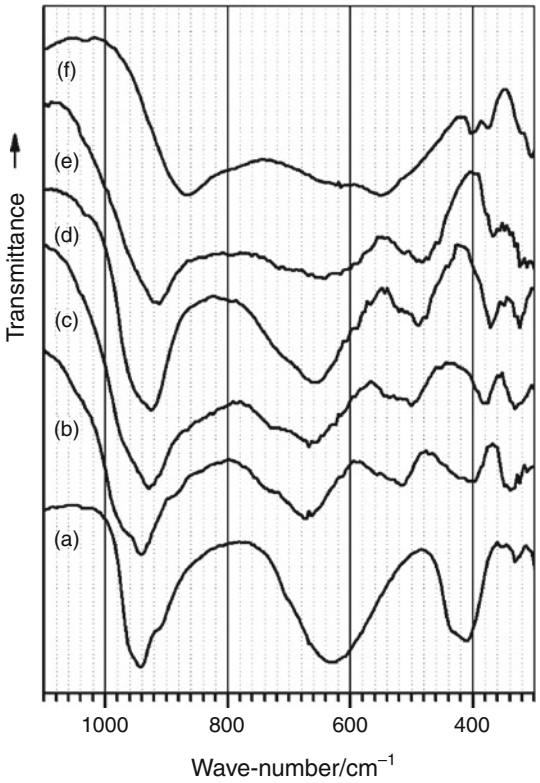

Fig. 4 IR spectra of: (*a*) $CoMoO_4$, (*b*) $Al_8V_{10}W_{16}O_{85}$, (*c*) $Fe_4Al_4V_{10}W_{16}O_{85}$, (*d*) $Fe_8V_{10}W_{16}O_{85}$ [12], (*e*) $Fe_8V_{10}W_{12}Mo_4O_{85}$ [14] and (*f*) ZnV_2O_6

The IR spectrum of the $Fe_8V_{10}W_{16}O_{85}$ (curve *d*) reveals the presence of absorption bands with their maxima at 922, 654, 486, 368, and 320 cm^{-1} [12–14]. With increasing the incorporation extent of the lighter and smaller Al^{3+} ions into the structure of $Fe_8V_{10}W_{16}O_{85}$ a relatively small shift of the respective absorption bands towardhigher wave-numbers was observed. Their maxima characteristic for $Al_8V_{10}W_{16}O_{85}$ are observed at 944, 660, 514, 412, and 334 cm^{-1} (curve *b*). A broad absorption bands lying at the range of wave-numbers 1,050–800 cm^{-1} are characteristic for all presented spectra (curves *a–f*) of phases built up only from distorted octahedra. It is noteworthy that broad absorption band in the IR spectrum of WO_3 covering the wave-number region of 1,000–700 cm^{-1} is caused by stretching vibrations of W–O bonds in highly distorted WO_6 octahedra [13, 14]. Thus, the absorption band covering the wave-number region of 1,050–800 cm^{-1} in the IR spectrum of the $Fe_8V_{10}W_{16}O_{85}$ type phases can be attributed to stretching vibrations of the very short M–O bonds in the MO_6 (M = W, V, Al, Fe) octahedra [19]. Another very broad absorption band covering the wave-number region of 800–550 cm^{-1} can correspond to stretching vibrations of longer M–O bonds in MO_6 octahedra. A similar absorption band with a 640 cm^{-1} maximum was noticed in an IR spectra of α- and γ-Fe_2WO_6, comprising

WO_6 and FeO_6 octahedra in their structures [13, 14, 25]. Next absorption band recorded in the range of 550–400 cm^{-1} can be the most likely ascribed to stretching vibrations of Fe–O and Al–O bonds in MO_6 octahedra. A similar absorption bands were noticed in the IR spectra of γ-Fe_2WO_6, $FeVO_4$, and $AlVO_4$ in the structure of which the FeO_6 or AlO_6 octahedra occur [7, 13, 14, 25]. On the other hand, bands lying within the wave-number range of 400–250 cm^{-1} may correspond to bending vibrations of M–O bonds in MO_6 octahedra or be of a mixed character [14, 19]. An evident broadening of the absorption bands in the IR spectrum of $Fe_8V_{10}W_{12}Mo_4O_{85}$ (curve *e*) in comparison to the IR spectrum of $Fe_8V_{10}W_{16}O_{85}$ is undoubtedly due to an appearance of numerous additional Mo–O bonds in the structure of $Fe_8V_{10}W_{12}Mo_4O_{85}$.

Thus, analysis of the IR spectra of the $Fe_8V_{10}W_{16}O_{85}$ type phases seems to support assumption based on structural considerations that these phases are built up from MO_6 octahedra.

Conclusions

In this study, the results concerning the quaternary system Fe_2O_3–Al_2O_3–V_2O_5–WO_3 were presented for the first time. The XRD, DTA, and IR measuring techniques were used to show that:

1. In the ternary system Al_2O_3–V_2O_5–WO_3 new compound $Al_8V_{10}W_{16}O_{85}$ forms, not described earlier in literature.
2. The $Al_8V_{10}W_{16}O_{85}$ melts incongruently at 1,183 K with deposition of $Al_2(WO_4)_3$ and WO_3 as a solid products of melting.
3. In the quaternary system Fe_2O_3–Al_2O_3–V_2O_5–WO_3 continuous solid solution $Fe_{8-x}Al_xV_{10}W_{16}O_{85}$ forms, not described earlier in the literature.
4. $Al_8V_{10}W_{16}O_{85}$ and $Fe_8V_{10}W_{16}O_{85}$ as well as solid solutions $Fe_{8-x}Al_xV_{10}W_{16}O_{85}$ and $Fe_8V_{10}W_{16-x}Mo_xO_{85}$ are isostructural with M–Nb_2O_5 and $(W_{0.35}V_{0.65})_2O_5$ and belong to block type structure phases.
5. With the increase of Al^{3+} content in the crystal lattice of $Fe_8V_{10}W_{16}O_{85}$ a decrease of the $a = b$ parameters of the unite cell occurs, with *c* parameter being almost constant.
6. The melting temperature of the $Fe_{8-x}Al_xV_{10}W_{16}O_{85}$ solid solution increase with increasing the content of Al_2O_3 and changes from being equal to 1,113 K for $x = 0$ up to 1,183 K for $x = 8$.
7. Analysis of the IR spectra of the $Fe_8V_{10}W_{16-x}Mo_xO_{85}$ type phases supports assumption that these phases are built up from VO_6, WO_6, FeO_6, and AlO_6 octahedra.

References

1. Eckert H, Wachs IE. Solid state ^{51}V NMR structural studies on supported vanadium(V) oxide catalysts: vanadium oxide surface layers on alumina and titania supports. J Phys Chem. 1989;93:6796–805.
2. Vuurman MA, Stufkens DJ, Oskam A, Deo G, Wachs IE. Combined Raman and IR study of MO_x–V_2O_5/Al_2O_5 (MO_x = MoO_3, WO_3, NiO, CoO) catalysts under dehydrated conditions. J Chem Soc Faraday Trans. 1996;92(17):3259–65.
3. Guerrero-Perez MO, Herrera MC, Malpartida I, Larrubia MA, Alemany LJ. Characterization and FT-IR study of nanostructured alumina-supported V–Mo–W–O catalysts. Catal Today. 2006;118:360–5.
4. Mitra B, Wachs IE, Deo G. Promotion of the propane ODH reaction over supported V_2O_5/Al_2O_3 catalyst with secondary surface metal oxide additives. J Catal. 2006;240:151–9.
5. Craig DC, Stephenson NC. A structural study in the system Al_2O_3–WO_3. Acta Cryst. 1968;B24:1250–5.
6. Hanuza J, Maczka M, Hermanowicz K, Andruszkiewicz M, Pietraszko A, Strek W, Deren P. The structure and spectroscopic properties of $Al_{2-x}Cr_x(WO_4)_3$ crystals in orthorhombic and monoclinic phases. J Solid State Chem. 1993;105:49–69.
7. Dabrowska G, Tabero P, Kurzawa MJ. Phase relations in the Al_2O_3–V_2O_5–MoO_3 system in the solid state. The crystal structure of $AlVO_4$. J Phase Equilib Differ. 2009;30(3):220–9.
8. Tarama K, Teranishi S, Yoshida S. Study on the reduction process of vanadium oxide catalysts by means of infrared spectroscopy and X-ray diffraction. Bull Inst Chem Kyoto Univ. 1968;5:185–97.
9. Darriet J, Galy J, Hagenmuller P. Mixed oxides of bronze structure $M_xV_{2-y}T_yO_5$ (T = Mo, W). I $Li_xV_{2-y}T_yO_5$. J Solid State Chem. 1971;3:596–603. (in French).
10. Walczak J, Rychlowska-Himmel I. Investigation of the real composition of the phase formed in the Fe_2O_3–V_2O_5–WO_3 system. J Mater Sci. 1994;29:2745–50.
11. Rychlowska-Himmel I. Phase equilibria in the system Fe_2O_3–V_2O_5–WO_3 in the solid state. J Therm Anal Calorim. 2000;60:173–6.
12. Walczak J, Rychlowska-Himmel I, Tabero P. Reaction mechanism of $Fe_8V_{10}W_{16}O_{85}$ synthesis. J Therm Anal Calorim. 1999;56:419–22.
13. Rychlowska-Himmel I, Tabero P. Phase equilibria in the system V_2O_5–$Fe_8V_{10}W_{16}O_{85}$ and some properties of the $Fe_8V_{10}W_{16}O_{85}$ phase. J Therm Anal Calorim. 2001;65:537–43.
14. Tabero P. Formation and properties of the $Fe_8V_{10}W_{16-x}Mo_xO_{85}$ type solid solution. J Therm Anal Calorim. 2007;88:37–41.
15. Walczak J, Rychlowska-Himmel I. Phase equilibria in the $Fe_8V_{10}W_{16}O_{85}$–Fe_2O_3 and $Fe_8V_{10}W_{16}O_{85}$–Fe_2WO_6 systems. J Therm Anal Calorim. 1998;54:867–72.
16. Walczak J, Rychlowska-Himmel I. Phase diagram of the $FeVO_4$–Fe_2WO_6 system. Thermochim Acta. 1994;239:269–74.
17. Blonska-Tabero A. New phase in the system $FeVO_4$–$Cd_4V_2O_9$. J Therm Anal Calorim. 2008;93:707–10.
18. Bosacka M, Blonska-Tabero A. Reinvestigation of system CdO–V_2O_5 in the solid state. J Therm Anal Calorim. 2008;93:811–5.
19. Tomaszewicz E, Typek J, Kaczmarek SM. Synthesis, characterization and thermal behaviour of new copper and rare-earth metal tungstates. J Therm Anal Calorim. 2009;98:409–21.
20. Filipek E, Wieczorek-Ciurowa K. Comparison between the synthesis in molybdenum and antimony oxides system by high-temperature treatment and high-energy ball milling. J Therm Anal Calorim. 2009;97:105–10.
21. Mertin W, Andersson S, Gruehn R. The crystal structure of M–Nb_2O_5. J Solid State Chem. 1970;1:419–24. (in German).

22. Israelsson M, Kihlborg L. $(W_{0.35}V_{0.65})_2O_5$, a new, simple block structure. Ark Kemi. 1968;30(12):129–40.
23. Andretti GD, Calestani G, Montenero A. Refinement of the crystal structure of ZnV_2O_6. Z Kristallogr. 1984;168:53–8.
24. Smith G, Ibers JA. The crystal structure of cobalt molybdate, $CoMoO_4$. Acta Cryst. 1965;19:269–73.
25. Senegas J, Galy J. Crystal structure of double oxide Fe_2WO_6. J Solid State Chem. 1974;10:5–11. (in French).